Available online at www.sciencedirect.com
SCIENCE DIRECT®
Physics Letters A 318 (2003) 184–191
PHYSICS LETTERS A
www.elsevier.com/locate/pla

Towards an atom interferometric determination of the Newtonian gravitational constant

M. Fattori, G. Lamporesi, T. Petelski, J. Stuhler, G.M. Tino *

Dipartimento di Fisica and LENS, Università di Firenze; INFN, Sezione di Firenze; Via Sansone 1, I-50019 Sesto Fiorentino (FI), Italy

Received 9 November 2002; accepted 27 July 2003

Communicated by V.M. Agranovich

Abstract

We report on progress towards an atom interferometric determination of the Newtonian gravitational constant. Free-falling laser-cooled atoms will probe the gravitational potential of nearby source masses. To reduce systematic errors, we will perform double differential measurements between two vertically separated atom clouds and with different source mass positions.

PACS: 04.80.-y; 39.20.+q; 03.75.Dg; 93.85

1. Introduction

The Newtonian gravitational constant G is—together with the speed of light—the most popular physical constant. Invented by Newton in 1686 to describe the gravitational force between two massive objects and first measured by Cavendish more than a hundred years later [1], "big G" became more and more subject of high precision measurements. There are many motivations for such measurements,[1] ranging from purely metrological interest over determinations of mass distributions of celestial objects to geophysical applications. In addition, many theoretical models profit from an accurate knowledge of G.

Despite these severe motivations and some 300 measurements in the past 200 years,[2] the 1998 CODATA [4] recommended value of $G = (6.673 \pm 0.010) \times 10^{-11}\ \mathrm{m^3\,kg^{-1}\,s^{-2}}$ includes an uncertainty of 1500 parts per million (ppm). Thus, G is still the least accurately known fundamental physical constant. Recently, two measurements with much smaller uncertainties of 13.7 ppm [5] and 41 ppm [6] have been reported. However, the given values for G still disagree on the order of 100 ppm. Therefore, it is useful to perform high resolution G-measurements with different methods. This may help to identify possible systematic effects. It is worthwhile to mention that so far, only few conceptually different methods have resulted in G measurements on the level of 1000 ppm or better [3]. All these methods have in common that the masses,

* Corresponding author.
E-mail address: tino@fi.infn.it (G.M. Tino).

[1] A comprehensive listing of motivations for G measurements can be found in Ref. [2].

[2] For a recent review of the status of G measurements, see, e.g., Ref. [3].

0375-9601/$ – see front matter
doi:10.1016/j.physleta.2003.07.011

which probe the gravitational field of external source masses, are suspended (e.g., with fibres). One way to exclude this possible source of systematic effects is to perform a free-fall experiment. A high precision measurement of G using a free-falling corner cube (FFCC) has already been performed [7] but the uncertainty remained on the order of 1400 ppm.

In order to surpass this result, we are setting up an experiment in which free-falling atoms are used to probe the gravitational acceleration originating from nearby source masses [8]. In this way, we will combine the powerful techniques of atom interferometry[3] and laser cooling.[4] Using atomic probe masses with well-known properties will further reduce and help to identify systematic effects.

In this Letter we firstly describe the general idea of a determination of the Newtonian gravitational constant based on free-falling atoms and atom interferometry. Then we present the setup and the current status of our experiment. Furthermore, we argue that our targeted accuracy of $\Delta G/G \propto 100$ ppm is reasonable.

2. General method

2.1. Free-fall gravity measurement

The basic idea of a free-fall experiment is the following: a falling object, accelerated by the earth's gravitational force, changes its vertical position $z(t)$ according to

$$z(t) = -\frac{1}{2}gt^2 + v_0 t + z_0, \tag{1}$$

$g = 9.81\ \mathrm{m\,s^{-2}}$, v_0 and z_0 being the acceleration on earth, the initial velocity and the starting position of the object. For simplicity, any spatial variation of g is omitted. To determine g, it is sufficient to measure three positions at distinct times $z(t_1)$, $z(t_2)$, $z(t_3)$ and then solve the system of equations.

A gravimeter—an apparatus that allows such a measurement of the vertical acceleration—can be extended to determine G. One adds source masses and measures by which amount they change the vertical acceleration g. Taking into account the mass distributions, one can then assign a value to G.

2.2. Atom interferometry and detection of vertical accelerations

State-of-the-art gravimeters, as used in [7], consist of a Michelson interferometer with a vertically aligned arm that has a FFCC as retro-reflecting mirror. The vertical movement of the FFCC can be derived from the interference signal. When dealing with atoms as probe masses, this technique is no longer applicable because scattering of laser light would disturb their free-fall dramatically.[5] The method of atom interferometry makes use of a unique advantage of atomic probe masses: the possibility of addressing and controlling their internal states. In the following, we describe how the so-called Raman type atom interferometry can be used to perform the position measurements, which are required to detect the vertical acceleration. For a more detailed description, refer to [11–13].

In a vertical Raman atom interferometer, free-falling atoms are illuminated by pulses of two laser beams with frequencies ω_1 and ω_2 (see Fig. 1a). The beams counterpropagate along the z-axis with wave vectors $\vec{k}_1 = k_1\vec{e}_z$ and $\vec{k}_2 = -k_2\vec{e}_z$ ($k_i = \omega_i/c$, $i = 1, 2$). ω_1 and ω_2 are close to transitions of a three-level atom in which two ground or metastable states $|a\rangle$ and $|b\rangle$ share a common excited state $|e\rangle$. During the pulses, the lasers drive two-photon Raman transitions between $|a\rangle$ and $|b\rangle$ that lead to Rabi oscillations: as illustrated in Fig. 1b, the probability of finding atoms in one specific state oscillates temporally between zero and one. A π-pulse, which is a pulse of duration $\tau = \pi/\Omega$, switches the atomic state coherently from $|a\rangle$ to $|b\rangle$ or vice versa. On the contrary, a $\pi/2$-pulse with duration $\tau = \pi/(2\Omega)$ splits the atom wave packet into an equal superposition of $|a\rangle$ and $|b\rangle$. Note that for given transitions, the characteristic Rabi frequency Ω depends only on the light parameters.

More precisely, the light field affects the atoms threefold: firstly, as already mentioned, the real ampli-

[3] For an overview on atom interferometry, see Ref. [9a] and references therein or Ref. [9b].

[4] A laser cooling overview can be found in the Nobel lectures of [10].

[5] The acceleration of ^{87}Rb atoms due to a 10 $\mathrm{W\,m^{-2}}$ laser resonant to the D2-line at 780 nm exceeds $10^4\ \mathrm{m\,s^{-2}}$.

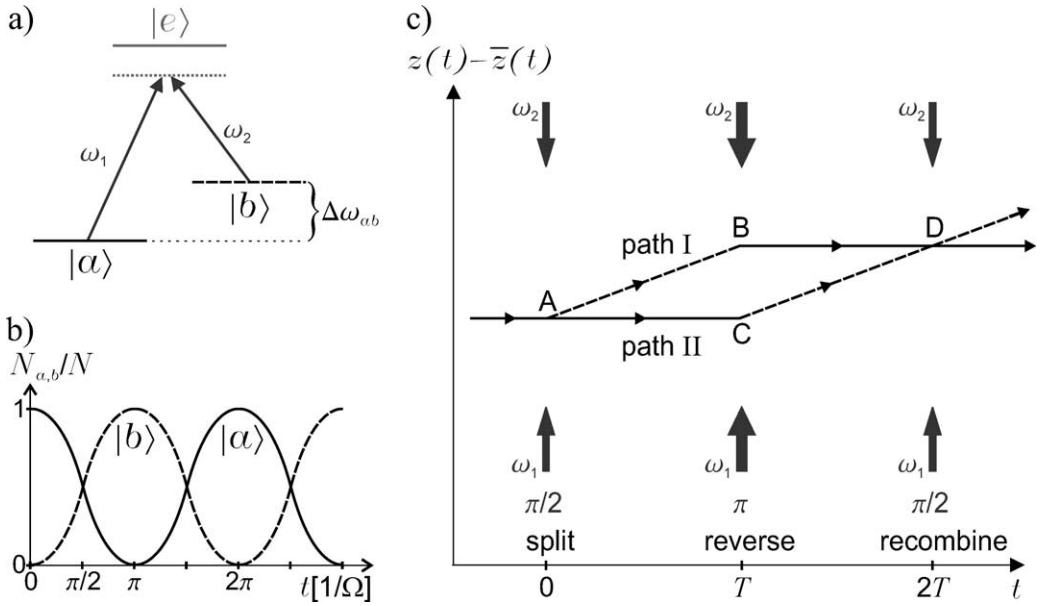

Fig. 1. Graphical illustration of the Raman atom interferometer. (a) Three-level atom with lower states $|a\rangle$ and $|b\rangle$ that share an excited state $|e\rangle$. The Raman lasers have frequencies ω_1, ω_2 slightly below the transition frequencies with a difference that matches the splitting $\Delta\omega_{ab}$ of the lower states. (b) Temporal evolution of the relative number $N_{a,b}/N$ of atoms in states $|a\rangle$ and $|b\rangle$ during the interaction with the Raman laser light field. Ω is the two-photon Rabi frequency and depends only on light parameters. (c) Scheme of the Raman interferometer. On the vertical axis we plot the atomic vertical position $z(t)$ after subtracting the free-fall trajectory $\bar{z}(t)$. Atom paths are split, reversed and recombined using Raman pulses (see text).

tudes α, β of the atomic wavefunction $\Psi = \alpha e^{i\Phi_\alpha}|a\rangle + \beta e^{i\Phi_\beta}|b\rangle$ change in time. Secondly, the phases $\Phi_{\alpha,\beta}$ are modified as listed in Table 1. These phase terms depend on the local phase $\phi_{\text{eff}}(z,t)$ of the light field seen by the atom and contain hence information about the vertical position of the atom.

$$\phi_{\text{eff}}(z,t) = k_{\text{eff}}(t)z - \int_0^t \omega_{\text{eff}}(\tau)\,d\tau - \phi(t), \qquad (2)$$

where $\phi(t)$ is a phase term that can be controlled externally and $k_{\text{eff}}(t) = \hbar(k_1(t) + k_2(t))$, $\omega_{\text{eff}}(t) = \omega_1(t) - \omega_2(t)$. Thirdly, if the atom changes its internal state, the two-photon Raman transition alters the atomic momentum by an amount of $\hbar k_{\text{eff}}$ due to the process of absorption and induced emission.

Applying first a $\pi/2$-pulse, then a π-pulse and finally another $\pi/2$-pulse, each separated by the time T, results in an interferometer configuration for the atoms. This Raman interferometer is shown schematically in Fig. 1c. The first pulse acts as a beam splitter for the atoms at point A. The atomic wave packet is split into an equal superposition of $|a, p\rangle$ and $|b, p+\hbar k_{\text{eff}}\rangle$ (p and $p+\hbar k_{\text{eff}}$ are the external momentum of the atom). The π-pulse at points B and C plays the role of the mirrors in a classical Michelson interferometer. It reverses the internal state of the atoms and modifies their momentum by $\pm\hbar k_{\text{eff}}$. The final $\pi/2$-pulse at point D acts as a second beam splitter. It recombines atoms with different paths (path I $= \overline{\text{ABD}}$, path II $= \overline{\text{ACD}}$). After recombination, the probability N_a/N of finding the atoms in state $|a\rangle$ shows a typical

Table 1
Effect of a Raman pulse. Atoms that change the state receive a momentum of $\pm\hbar k_{\text{eff}}$ and a position and time dependent phase factor. Contributions to the phase factor that do not depend on position or time are neglected because they do not contribute to the interference signal (details can be found in [12]). See Eq. (2) for the definition of $\phi_{\text{eff}}(z,t)$

Internal state	Momentum	Phase factor Φ
$\|a\rangle \to \|b\rangle$	$p \to p + \hbar k_{\text{eff}}$	$\phi_{\text{eff}}(z,t)$
$\|b\rangle \to \|a\rangle$	$p + \hbar k_{\text{eff}} \to p$	$-\phi_{\text{eff}}(z,t)$
$\|a\rangle \to \|a\rangle$	$p \to p$	0
$\|b\rangle \to \|b\rangle$	$p + \hbar k_{\text{eff}} \to p + \hbar k_{\text{eff}}$	0

interference-like behaviour:

$$N_a/N \propto 1 + \cos(\Phi_{\mathrm{I}} - \Phi_{\mathrm{II}}). \tag{3}$$

$\Phi_{\mathrm{I,II}}$ are the phases accumulated on path I and II, respectively, and with $|a\rangle$ as final internal state. Taking the phase values listed in Table 1 and considering the atomic trajectories shown in Fig. 1 as well as the pulse timing one finds:

$$\Phi_{\mathrm{I}} = \phi_{\mathrm{eff}}(z_{\mathrm{A}}, 0) - \phi_{\mathrm{eff}}(z_{\mathrm{B}}, T), \tag{4}$$

$$\Phi_{\mathrm{II}} = \phi_{\mathrm{eff}}(z_{\mathrm{C}}, T) - \phi_{\mathrm{eff}}(z_{\mathrm{D}}, 2T), \tag{5}$$

where T is the time between two sequent pulses.

Free-falling atoms are accelerated during the interferometer time $2T$. In the laboratory frame, this leads to a variation of their transition frequencies due to the first order Doppler effect. As a consequence, for a proper functioning of the pulse sequence, we vary $\omega_{\mathrm{eff}}(t)$ linearly in time, exactly as the velocity of the atoms does.

Taking $\omega_{\mathrm{eff}}(t) = \omega_{\mathrm{eff}}(0) - \gamma t$, neglecting variations of k_{eff} and using Eq. (1) for the determination of z_{A}, z_{B}, etc. we find

$$\Phi_{\mathrm{I}} - \Phi_{\mathrm{II}} = (\gamma - k_{\mathrm{eff}} g)T^2 - \phi(0) + 2\phi(T) - \phi(2T). \tag{6}$$

Assuming proper Doppler effect compensation ($\gamma = k_{\mathrm{eff}} g$) and no perturbation of the laser phase evolution, one is left with $\Phi_{\mathrm{I}} - \Phi_{\mathrm{II}} = 0$ (all atoms in state $|a\rangle$). Actively changing the laser phase between T and $2T$ by $\delta\phi$ will result in $\phi(2T) = \phi(0) + \delta\phi = \phi(T) + \delta\phi$ and hence $\Phi_{\mathrm{I}} - \Phi_{\mathrm{II}} = -\delta\phi$. In this way, one can scan the interference fringe to prove $(\gamma - k_{\mathrm{eff}} g) = 0$ (for right γ) or reveal the phase offset $(\gamma - k_{\mathrm{eff}} g)T^2$ for imperfect Doppler compensation. In both cases, the value of g is obtained combining the measured phase offset and the value γ, which is set by a frequency generator. Note that this interferometer scheme is—in the case of a uniform acceleration—insensitive to the initial condition of the atom. As the acceleration induced signal is proportional to T^2 (see first term in Eq. (6)), an improvement of the gravimeter sensitivity can be obtained increasing the length of the atomic trajectories as far as possible. For a given extent of the apparatus, by launching the atoms vertically (atomic fountain) instead of just releasing them, it is possible to increase T by a factor of 2. The power of a gravimeter based on vertical Raman atom interferometry has already been demonstrated with Cs atoms in a determination of g with an accuracy of $\Delta g/g \approx 10^{-8}$ and a sensitivity 10 times better [14].

2.3. Atom interferometric G-measurement

The modification of the vertical Raman atom interferometer that allows to measure G is the same as already mentioned in Section 2.1. Like in [7], one adds well-known source masses (SM) close to the atomic trajectories. The change of the local acceleration due to the gravitational potential of the SM can be measured and depends only on the SM density distribution as well on G. However, even quite heavy SM (e.g., 1 ton of tungsten) are able to generate only an acceleration on the order of $10^{-7} g$. As a consequence, for a targeted accuracy in G of 10^{-4}, the use of a simple Raman atom interferometer requires a control of the systematic errors at the level of $10^{-11} g$. At the moment this is an impossible task, considering all the effects that limit the present atomic gravimeter at the $10^{-8} g$ level [12].

To be able to perform a high precision measurement of G, we consequently have to extend the atom gravimeter in two ways.

Firstly, we will launch two clouds of atoms to realize two fountains that are displaced vertically (Fig. 2, clouds 1 and 2). The Raman lasers will then act on both clouds simultaneously and generate two interferometers at the same time. In a detection of the differential phase shift between the two interferometers, spatially homogeneous accelerations cancel (e.g., earth's gravity acceleration g that changes due to tides, pressure variations, etc.) and common mode measurement errors are reduced (e.g., uncontrolled phase variation in the Raman beams). The two-clouds setup results in an atomic gradiometer [15]. In addition, the signal due to the SM can be increased by a proper choice of the atomic trajectories. If the trajectory of the upper cloud is located above the SM, this cloud will experience a SM induced acceleration in the direction of the earth acceleration (in $-z$ direction). In contrast, if the lower cloud is located below the SM, its SM induced acceleration will be in $+z$ direction. The difference of these two accelerations results in a signal that is twice the one achievable with only one cloud.

This differential measurement has another big advantage. The one cloud interferometer signal is

$k_{\text{eff}}(g + a)T^2$ where a is the SM induced acceleration. It is dominated by g, which is about 7 orders of magnitude bigger than a. Therefore, to measure a and consequently G with an accuracy of 10^{-4}, one needs to know k_{eff} and T^2 better than 10^{-11}. But in a two cloud differential measurement, g cancels and the experimental requirements (knowledge of the pulse timing T, the laser frequency and the laser beam alignment) reduce by a factor of 10^7.

As a second modification of the gravimeter scheme, the SM will be moved in a way similar to the one described in [16]. We will determine the differential phase shifts of the two atom clouds with the SM in position 1 and with the SM in position 2 (see Fig. 2). Evaluating the difference between those measurements will further reduce systematic effects. In this way, also systematic errors due to spatially inhomogeneous spurious accelerations are suppressed, if they are constant on the time scale of the SM repositioning. The most obvious example for such a removable systematic error is the effect of the earth's gravity gradient g'. This scheme is also able to remove phase-shifts arising from magnetic or electric fields that may be not homogeneous in space and phase-shifts caused by inertial forces. An example for the latter is the Coriolis force, which results in a phase offset if the atom trajectories and laser beams are not perfectly vertical.

3. Experimental setup

The described experiment is an ongoing project under the name MAGIA ("Misura Accurata di G mediante Interferometria Atomica"). A detailed description of the whole apparatus would go beyond the scope of this Letter. Hence, we will concentrate on some essential parts of the setup that ease the understanding of the measurement procedure. A more detailed description of the experimental setup will be published elsewhere [17].

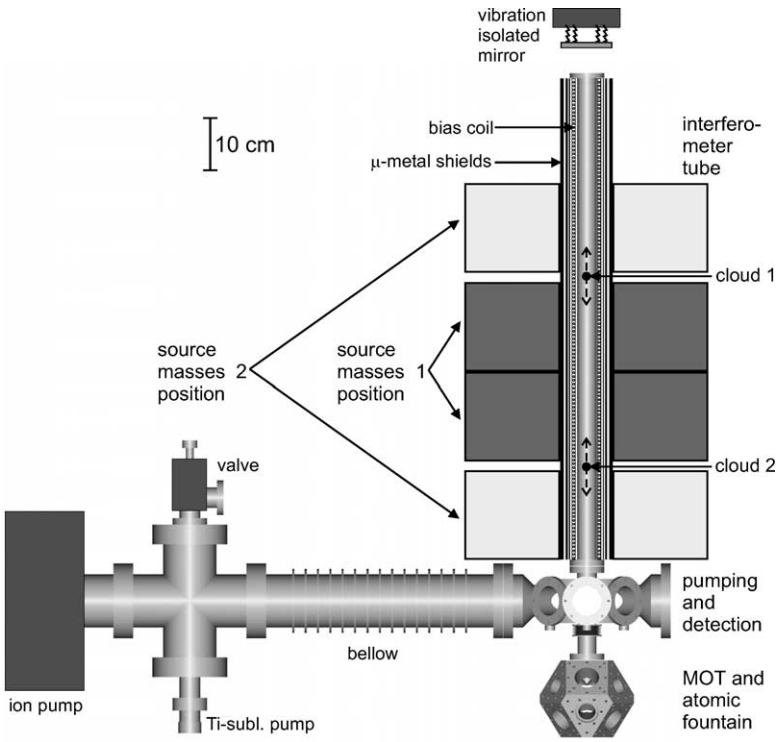

Fig. 2. Graphical illustration of the experimental setup with the vacuum system, the atomic trajectories and the source mass positions. Not included are the laser systems, the detection units and the source mass holder. The atomic trajectories during the time of the interferometer pulse sequence is sketched (dashed arrows).

3.1. Laser systems

The experiment will be performed using ^{87}Rb atoms, mainly because laser systems[6] and techniques for trapping, launching and detection of this element are nowadays standard. In our experiment, we use grating stabilized diode lasers that are locked to atomic transitions and amplified using standard techniques. Frequency modification and amplitude control of the laser light is achieved using acusto-optic modulators.

A critical part of the atom interferometer experiment are the lasers used to realize the Raman pulses because the relative phase between these two lasers is used as a ruler to measure the free-fall of the atoms. Uncontrolled variations of this relative phase will show up as noise in the acceleration measurement and could limit the precision of the G-determination. The Raman lasers are also grating stabilized laser diodes; but we have set up an optical phase-lock loop (OPLL) [18] to avoid random variations of their relative phase: the beat note of the two lasers is mixed down to low frequencies. The resulting signal is proportional to the phase difference between the two lasers and is used to stabilize their relative phase.

3.2. Vacuum system

The vacuum system is shown in Fig. 2 together with the source mass positions and the atomic trajectories. It mainly consists of three parts. The lowest part, a titanium cube with cut edges, is used to trap, cool and launch atoms that are evaporated from Rb dispensers. Six independent laser beams are needed to trap the atoms in a magneto-optical trap and to launch them in moving optical molasses. These beams are chosen to be in a 1–1–1 6-beam-σ^+/σ^- configuration. This keeps the central vertical axis free for the Raman laser beams and allows to realize a stable and precise atomic fountain [19].

The second part of the vacuum system is a stainless steel cell. It is used for pumping and detection of the atoms. Furthermore, it provides optical access to implement degenerate Raman cooling [20], a method to increase the brightness of the atomic fountain.

The upper part of the vacuum system consists of the interferometer tube which is made of titanium. The Raman laser beams enter the vacuum system from below at the central axis of the lower cube, leave the interferometer tube at the top, pass a $\lambda/4$ plate and are retro-reflected by a vibration isolated mirror. The Raman interferometer pulse sequence is applied while the atoms are on their free-fall parabola within this interferometer tube.

3.3. Source masses

The SM are planned to be two separate major discs of a tungsten alloy with a central hole. Each major disk will consist of several independent discs, located concentrically on top of each other. It will have an inner diameter of ~ 0.10 m, an outer diameter of ~ 0.44 m, a height of ~ 0.18 m and a mass of about 500 kg.

4. Targeted accuracy

In order to achieve an accuracy of $10^{-11}g$ in a free fall gravity measurement on earth, one has to know the vertical position of the probe masses within 30 μm. This restriction is caused by the vertical gravity gradient $g' = 3 \times 10^{-7} g\,\mathrm{m}^{-1}$ on earth. Because such a precise knowledge is very difficult to achieve with atomic fountains, we propose the following solution.

The SM in position 1 (Fig. 2, dark grey boxes) generate a vertical acceleration $a(z)$ on the central axis as plotted in Fig. 3a with a maximum of $a_{\max} \approx 10^{-6}\ \mathrm{m\,s}^{-2}$. Taking into account the earth gravity gradient g', $a(z)$ changes significantly (Fig. 3b). As indicated in this plot, we choose atomic trajectories which include an extremum of the overall acceleration where g' is compensated by the gradient of the SM induced acceleration. In this way, the resulting atomic phase shift is much less sensitive to the initial conditions (atomic position and velocity). Moving the source masses to position 2 (Fig. 2, light grey boxes) the sign and the amount of the SM-induced acceleration change, but the atomic trajectories remain located around an extremum of the acceleration. Hence,

[6] All the lasers used in the experiment are close to transitions from the two lowest hyperfine states $5^2S_{1/2}$, $F = 2$ and $5^2S_{1/2}$, $F = 3$ of ^{87}Rb to the $5^2P_{3/2}$, $F = 0, 1, 2, 3$ manifold. The corresponding wavelengths are around 780 nm.

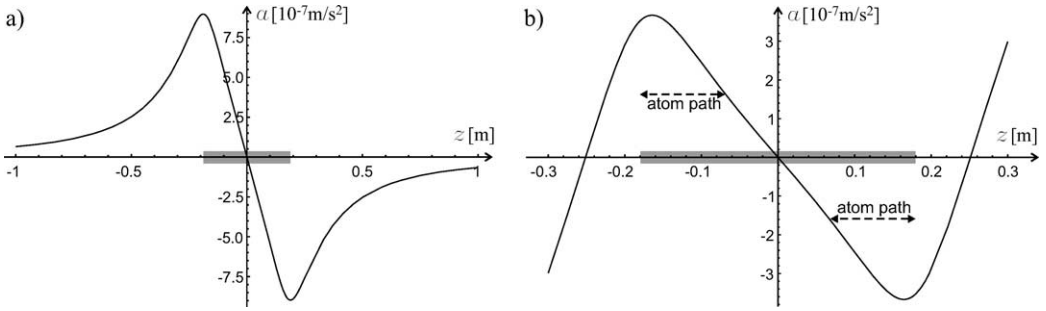

Fig. 3. Calculated on axis vertical acceleration $a(z)$ with the two 500 kg source masses in position 1 (see Fig. 2). The grey boxes illustrate the vertical position of the source masses. (a) $a(z)$ without g and g'. (b) $a(z)$ with g' included. The dashed arrows mark the projected atomic trajectories.

the atomic phase shift is again insensitive to variations of the initial conditions. To determine the effect of such variations quantitatively, we have performed numerical simulations [17]. Here we briefly describe our analysis and summarize the results.

First of all, we calculate the atomic trajectories for two clouds of atoms that are accelerated by g, g' and the SM. We assume a time $T = 150$ ms between two Raman pulses, which corresponds to an atomic free-fall height of ~ 0.11 m. The trajectories depend on the initial atomic conditions (atomic positions $z_{0,i}$ and velocities $v_{0,i}$ at the time $t = 0$ of the first Raman pulse; $i = 1, 2$ is numbering the clouds). The knowledge of the spacetime points of the atoms lets us determine the phases that are imprinted onto the atomic wave functions by the Raman pulses. The next step is to evaluate the interferometer phase shift $\Phi_i = \Phi_{\mathrm{I},i} - \Phi_{\mathrm{II},i}$ (see Eqs. (4) and (5)). Performing this analysis for different sets of parameters we find the optimum SM positions 1 and 2 as well as the atomic initial conditions that leave Φ_i relatively insensitive to variations in $z_{0,i}$ and $v_{0,i}$. Note that we use the same initial atomic conditions for both SM positions. This eases the experimental procedure because the launch of the atoms has not to be modified. Then we calculate $\Phi = \Phi_1 - \Phi_2$, the differential phase shift of the two interferometers (two clouds). Finally, we take the difference of the differential phase shifts Φ obtained with the two different SM positions. This phase difference is $\Delta\Phi \approx 0.9$ rad for the presented experimental conditions and depends linearly on G. Determining $\Delta\Phi$ within 1% per measurement and averaging 10 000 measurements, which corresponds to a data collection time of several hours, will allow a resolution of $\Delta G/G \approx 10^{-4}$.

The choice of the atomic trajectories around an extremum of the overall acceleration dramatically reduces the sensitivity to variations of initial atomic conditions. For example, to reach 100 ppm accuracy, the initial position and velocity of the atoms have only to be exact within ± 0.75 mm and ± 5 mm s^{-1}, respectively. This can be achieved in atomic fountains. However, the reduced sensitivity to initial atomic conditions comes at the price of a precise knowledge of the distance between the SM (0.01 mm) and accurate relative movement of the SM (to 0.1 mm). Although quite demanding, controlling and measuring source mass positions to this accuracy can be done.

For completeness we remember that the 1% precision in the $\Delta\Phi$ measurement requires some extra conditions. The Raman pulses must be short enough and consequently large enough in the frequency domain in order to really be $\pi/2$ and π pulses for all the detected atoms, even if they have different velocities. Moreover, the Raman beams have to be large enough in order to have a homogeneous power over the region occupied by the atoms. Finally, the detection system to measure the number of atoms in the upper and in the lower state has to provide a signal to noise ratio of 1000. Using 10^6 atoms this requires quantum projection noise limited detection [22]. The experimental apparatus has been designed in order to fulfil all these requirements. Not accomplishing these conditions will cause a reduced visibility of the fringes and a longer integration time to achieve the targeted 10^{-4} precision in G measurement. For

a more exhaustive description of these aspects refer to [12,21].

5. Conclusion

We presented a scheme that allows to measure the Newtonian gravitational constant G using a new method based on atom interferometry. In this scheme, free-falling atoms probe the gravitational potential of nearby source masses. Using two atom clouds in a gradiometer configuration and repeating measurements with different positions of the source masses reduce noise and systematic errors. We reported on the progress of our MAGIA experiment, which—based on the described scheme—aims at the high precision measurement of G. The experimental setup is in great part already functioning. We numerically analyzed the influence of atomic initial conditions and source mass locations on the measurement. The results are encouraging to determine G to the targeted accuracy of 100 ppm. Using modified configurations, atom interferometry can also be applied to prove the $1/r^2$-dependence of Newton's law of gravitation or to test the equivalence principle.

Acknowledgements

We thank Mark Kasevich for stimulating discussions and appreciate fruitful suggestions of Achim Peters and James Faller. J.S. and T.P. acknowledge support from the European Union under contract number HPRI/CT/1999/00111. This work is financed by the Istituto Nazionale di Fisica Nucleare (INFN).

References

[1] H. Cavendish, Philos. Trans. R. Soc. 88 (1798) 467.
[2] G.T. Gillies, Rep. Prog. Phys. 60 (1997) 151.
[3] J. Luo, Z.-K. Hu, Class. Quantum Grav. 17 (2000) 2351.
[4] P.J. Mohr, B.N. Taylor, Rev. Mod. Phys. 72 (2000) 351, the values can also be found at http://physics.nist.gov/cuu/Constants/index.html.
[5] J.H. Gundlach, S.M. Merkowitz, Phys. Rev. Lett. 85 (2000) 2869.
[6] T.J. Quinn, C.C. Speake, S.J. Richman, R.S. Davis, A. Picard, Phys. Rev. Lett. 87 (2001) 111101.
[7] J.P. Schwarz, D.S. Robertson, T.M. Niebauer, J.E. Faller, Science 282 (1998) 2230.
[8] G.M. Tino, A relativistic space time odyssey, in: I. Ciufolini, et al. (Eds.), Experiments and Theoretical Viewpoints on General Relativity and Quantum Gravity, Proceedings of the 25th Johns Hopkins Workshop on Current Problems in Particle Theory, Firenze, Italy, 2001, World Scientific, Singapore, 2001.
[9] (a) P.R. Berman (Ed.), Atom Interferometry, Academic Press, New York, 1997;
(b) D.E. Pritchard, A.D. Cronin, S. Gupta, D.A. Kokorowski, Ann. Phys. (Leipzig) 10 (2001) 35.
[10] S. Chu, Rev. Mod. Phys. 70 (1998) 685;
C.N. Cohen-Tannoudji, Rev. Mod. Phys. 70 (1998) 707;
W.D. Phillips, Rev. Mod. Phys. 70 (1998) 721.
[11] B. Young, M. Kasevich, S. Chu, in: Atom Interferometry, Academic Press, New York, 1997, p. 363.
[12] A. Peters, Dissertation, Department of Physics, Stanford University, 1998;
A. Peters, K.Y. Chung, S. Chu, Metrologia 38 (2001) 25.
[13] D.S. Weiss, Dissertation, Department of Physics, Stanford University, 1993.
[14] A. Peters, K.Y. Chung, S. Chu, Nature 400 (1999) 849.
[15] M.J. Snadden, J.N. McGuirk, P. Bouyer, K.G. Haritos, M.A. Kasevich, Phys. Rev. Lett. 81 (1998) 971.
[16] J. Schurr, F. Nolting, W. Künding, Phys. Rev. Lett. 80 (1998) 1142.
[17] J. Stuhler, M. Fattori, T. Petelski, G.M. Tino, in preparation.
[18] G. Santarelli, A. Clairon, S.N. Lea, G.M. Tino, Opt. Commun. 104 (1994) 339.
[19] K. Gibble, S. Chu, Phys. Rev. Lett. 70 (1993) 1771, and references therein.
[20] P. Treutlein, K.Y. Chung, S. Chu, Phys. Rev. A 63 (2001) 051401.
[21] J.M. McGuirk, G.T. Foster, J.B. Fixler, M.J. Snadden, M.A. Kasevich, Phys. Rev. A 65 (2002) 033608.
[22] G. Santarelli, Ph. Laurent, P. Lemond, A. Clairon, A.G. Mann, S. Chang, A.N. Luiten, C. Salomon, Phys. Rev. Lett. 82 (1999) 4619.